

Dislocation arrangements in cyclically deformed Au single crystal

P. Li*, S.X. Li, Z.G. Wang, Z.F. Zhang*

Shenyang National Laboratory for Materials Science, Institute of Metal Research, Chinese Academy of Sciences, 72 Wenhua Road, 110016 Shenyang, PR China

ARTICLE INFO

Article history:

Received 25 March 2010

Received in revised form 1 June 2010

Accepted 14 June 2010

Keywords:

Au single crystal
Cyclic deformation
Persistent slip bands
Dislocation arrangements

ABSTRACT

Cyclic deformation was carried out on $[2\bar{2}2]$ Au single crystal at plastic resolved strain amplitudes of 1.11×10^{-3} and 2.22×10^{-3} with a cyclic saturation stress of 23.4 MPa. Persistent slip bands (PSBs) were also found in the cyclically saturated specimens. In comparison with the fatigue-induced dislocation arrangements of other fcc metals, such as Cu, Ni and Ag, two basic criteria for determining whether the ladder-like PSBs form or not were proposed. Besides PSBs, the vein, wall and labyrinth structure also appeared in cyclically deformed $[2\bar{2}2]$ Au single crystals. Experimental results show that cyclic deformation behaviors of Au single crystals are very similar to those of Cu, Ni and Ag single crystals, which will become the important and fundamental basis to determine the cyclic deformation mechanism of fcc single crystal.

© 2010 Elsevier B.V. All rights reserved.

1. Introduction

Thompson et al. [1] firstly used a term “persistent slip bands” (PSBs) to call those slip bands (SBs) which reappeared at the old sites when the specimen was fatigued again after the previously formed slip bands had been polished away. Later, Winter [2] in 1974 and Finney and Laird [3] in 1975 separately discovered the plateau in the cyclic stress–strain (CSS) curve of Cu single crystals and proposed a two-phase model of dislocation structures to explain the formation of the plateau. Mughrabi [4] further performed constant plastic strain amplitudes tests on Cu single crystals over a wide range of amplitude and identified the lower strain limit of the plateau, and then obtained a well-documented CSS curve which clearly demonstrated three regions A, B and C. In region B, the plastic strain is mainly localized in the narrow PSBs and as the strain amplitude γ_{pl} increases, the volume fraction of the PSB's increases accordingly [2,3,5,6]. The plateau stress of Cu single crystals at room temperature is approximately in the range 27–30 MPa. However, it should be indicated that the plateau stress has a slight variation, e.g., Neumann obtained a saturation stress of 32 MPa [7]. This kind of variation was explained by Yan et al. [8] as a test start phenomenon and a frequency effect.

In addition to Cu single crystals, Ni single crystals could be regarded as the second fcc metallic crystal of which the cyclic deformation behaviors was investigated widely. Mughrabi et al. [9] indicated that the CSS curve of single-slip oriented Ni single

crystal exhibited similar three stages and a higher plateau stress of about 52 MPa as compared with that of Cu single crystal. Later, Blochwitz and Veit [10] found that the volume fraction of PSBs increased with the increment of the applied strain amplitude and confirmed again the three-stage character of the CSS curve in Ni single crystal with single-slip orientation, which are consistent with those of Cu single crystals. As one of the typical fcc metals, Ag single crystals were rarely investigated to show its cyclic deformation behaviors. Mughrabi et al. [9] found that the characteristic thresholds for the formation of a PSB-ladder structure at room temperature, expressed as τ_s/G , had a very similar value of $(6.55 \pm 0.5) \times 10^{-4}$ for Cu, Ni and Ag single crystals. Recently, after systematically studying the cyclic deformation behaviors of differently oriented Ag single crystals [11–14], we found that the CSS curve of single-slip oriented Ag single crystal also showed a clear plateau feature with a plateau stress of about 20 MPa and the corresponding PSBs are quite similar to those found in Cu and Ni single crystals.

Likewise, Au is another typical fcc simple metal, but so far there is no public report on the cyclic deformation behavior of Au single crystals. Therefore, in this study, Au single crystal is for the first time selected as a model material for cyclic deformation in order to establish its CSS behavior and to observe the related dislocation structure. Together with the well-known results in Cu, Ni and Ag single crystals, it will become possible to find the general law of cyclic deformation behavior, especially the evolution of fatigue-induced dislocation arrangements. The ultimate goal is to explore the physical nature behind the law, which in return determines the necessity of the investigation on cyclic deformation behavior of Au single crystal as a missing link.

* Corresponding authors. Tel.: +86 24 23971043; fax: +86 24 23891320.
E-mail addresses: pli@imr.ac.cn (P. Li), zhfzhang@imr.ac.cn (Z.F. Zhang).

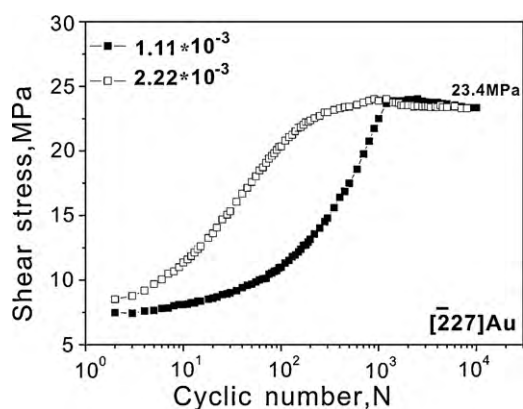


Fig. 1. Cyclic hardening curves of $[\bar{2} 2 7]$ Au single crystal at different plastic strain amplitudes.

2. Experimental procedures

A bulk Au single crystal plate was firstly grown from electrolytic Au of 99.999% purity by the Bridgman method. Secondly, fatigue specimens of 6 mm × 5 mm × 16 mm in gauge section and 54 mm in total length were made by an electrospark cutting machine. The orientation of the specimen was determined by the electron back-scattering diffraction (EBSD) technique in a Cambridge S360 scanning electron with the accuracy within $\pm 2^\circ$. Here, the stress axis orientation of the Au single crystal can be referred to as $[\bar{2} 2 7]$ with a Schmid factor of about 0.451. Before fatigue tests, all the specimens were electro-polished to produce a strain-free and mirror-like surface for microscopic observations. In the process of loading, the errors in aligning the specimens within the loading axis are minimized to $\pm 1^\circ$. Then the cyclic deformation tests were performed in symmetric push–pull loading at room temperature in air using a Shimadzu servo-hydraulic fatigue testing machine. A triangular waveform signal with a frequency of 0.5 Hz was used for the total strain control with limitation of plastic strain. All specimens were deformed cyclically up to the occurrence of saturation. After fatigue tests, the surface slip morphologies and the dislocation configurations were carefully observed by the scanning electron microscope (SEM) and the electron channeling contrast (ECC) technique, respectively.

3. Results and discussion

Fig. 1 shows the cyclic hardening curves of $[\bar{2} 2 7]$ Au single crystal cyclically deformed at the plastic shear strain amplitudes of $\gamma_{pl} = 1.11 \times 10^{-3}$ and $\gamma_{pl} = 2.22 \times 10^{-3}$, respectively. It can be seen from Fig. 1 that although the cyclic hardening rates are different at different strain amplitudes, the saturation resolved shear stress is about 23.4 MPa, at both $\gamma_{pl} = 1.11 \times 10^{-3}$ and $\gamma_{pl} = 2.22 \times 10^{-3}$, which suggests at least in the strain range of 1.11×10^{-3} to 2.22×10^{-3} the CSS curve of Au single crystal also shows a plateau behavior. It is interesting to note that the plateau stress of Au single crystals is located between those of Cu and Ag single crystals ($\tau_s^{Cu} = 28$ MPa, $\tau_s^{Ag} = 18$ MPa), which is well consistent with the

variation of stacking fault energy (SFE) of these three fcc metals (see Table 1). According to the characteristic thresholds τ_s/G for the formation of a PSB-ladder structure proposed by Mughrabi et al. [9], the corresponding value of Au single crystal can be determined to be $\tau_s^{Au}/G \approx 8.7 \times 10^{-4}$. Compared with the threshold values in Cu, Ni and Ag (see Table 1), this parameter of Au single crystals is slightly higher.

Fig. 2 presents the surface slip morphologies and dislocation patterns in $[\bar{2} 2 7]$ Au single crystal cyclically deformed at relatively low strain amplitude $\gamma_{pl} = 1.11 \times 10^{-3}$. The slip bands (SBs) are visible and evenly distributed on the surface, as shown in Fig. 2(a) and (b), which is almost the same as those of Cu and Ag single crystals [11]. Some PSBs with white trace are clearly seen in the matrix of Au single crystal, as shown in Fig. 2(c). These PSBs firstly observed in Au single crystal look like those found in Cu, Ni and Ag single crystals [14], which will contribute to a better understanding of the cyclic deformation mechanism of fcc single crystals. By Comparing Fig. 2(a) and (c), it is found that only a part of SBs displays the persistent characteristic; therefore, strictly speaking, the SBs should be divided into persistent and non-persistent ones, which is in accordance with the definition of PSBs by Thompson et al. [1]. Besides the PSBs, the vein also appears in Au single crystal, as shown in Fig. 2(d), the vein as part of the matrix is regularly separated by the channels [15]. The width of both the vein and channel is about 1.4 μm . The vein is composed of the dipole with positive–negative dislocations captured with each other [16]. After cyclic saturation at this strain amplitude, the vein pattern will further evolve and form the ladder-like PSB-ladder, which is found in $[\bar{2} 2 7]$ Au single crystal cyclically deformed at $\gamma_{pl} = 2.22 \times 10^{-3}$.

As shown in Fig. 3(a) and (b), the surface morphology of the cyclically saturated Au single crystal is characterized by the interactions between the primary and secondary SBs, which is also in line with the cases observed in Cu and Ag single crystals [11]. However, Au single crystals present some subtle differences in detail. As shown in Fig. 3(b), under the action of the secondary SBs, the primary SBs show a certain degree of distortion, which was not found in Cu and Ni single crystal with the same interaction between the primary and secondary SBs. Actually the distortion is more similar to some morphologies found in Al single crystals [17]. An initial opinion believes that the formation of distortion is related to the difference in their shear modulus. Compared with Ni, Cu and Ag, the shear modulus of Au and Al are significantly lower, which may endow them with more rheological properties in the deformation process and results in the appearance of the distortion.

At the strain amplitude $\gamma_{pl} = 2.22 \times 10^{-3}$, not only classical vein and PSB-ladder structures form (see Fig. 3(c) and (d)), but also the wall and labyrinth structures appear in $[\bar{2} 2 7]$ Au single crystal (see Fig. 3(e) and (f)), respectively. Firstly, Fig. 3(c) presents both the well-developed vein and PSB-ladder structures. So-called PSB ladders are composed of the regularly spaced rungs and the channels between the rungs (see Fig. 3(d)). In the cyclically deformed Cu, Ni and Ag single crystals, the volume fraction of the rungs in a PSB is about 10%, the thickness of ladder wall is roughly 0.1–0.2 μm and the channel width is about 1.2 μm [12]. Similar geometric parameter values of PSB-ladder structure are obtained from the cyclically deformed of Au single crystal. Secondly, Fig. 3(e) and (f) shows two other more complex dislocation patterns – PSB-

Table 1

Cyclic deformation behaviors (including saturation stress and PSB ladders formation) and physical parameters of Ni, Cu, Au and Ag single crystals at room temperature. Except for Au single crystal, the other data were quoted from extensive researches [4,9,12,20–24].

Metals	SFE γ_{sf} (mJ/m ²)	G [GPa]	Saturation stress τ_s (MPa)	G/γ_{sf} (10^{12} m ⁻¹)	τ_s/G (10^{-4})	Plateau behavior and PSB-ladder formation
Ni	80	76	50–52	~1.0	6.6	Yes
Cu	40	44	28–30	~1.1	6.4	Yes
Au	32	27	23–24	~0.84	8.7	Yes
Ag	16	30	18–20	~1.9	6.7	Yes

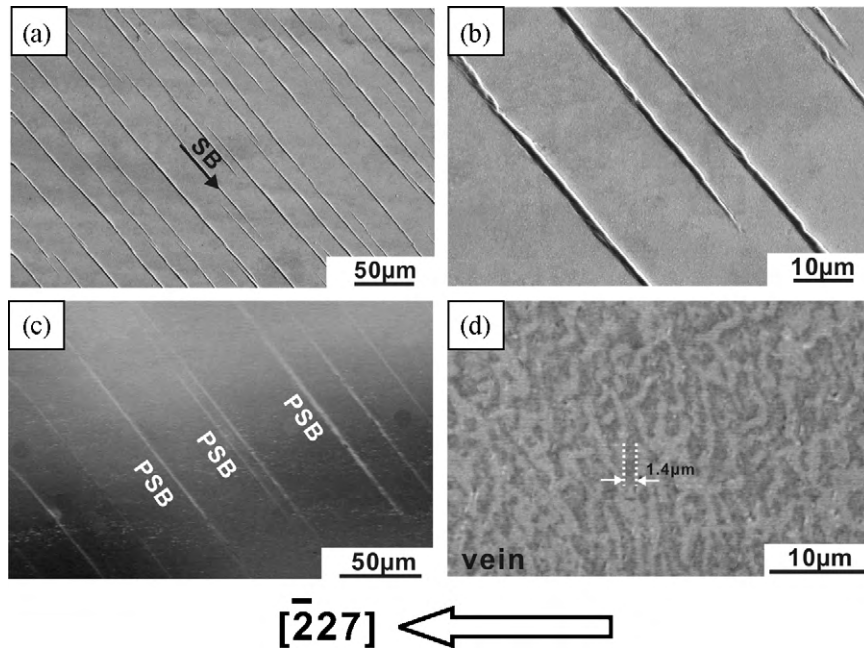


Fig. 2. Surface slip morphologies and dislocation patterns of $[\bar{2} 27]$ Au single crystal cyclically deformed at the strain amplitude of $\gamma_{pl} = 1.11 \times 10^{-3}$.

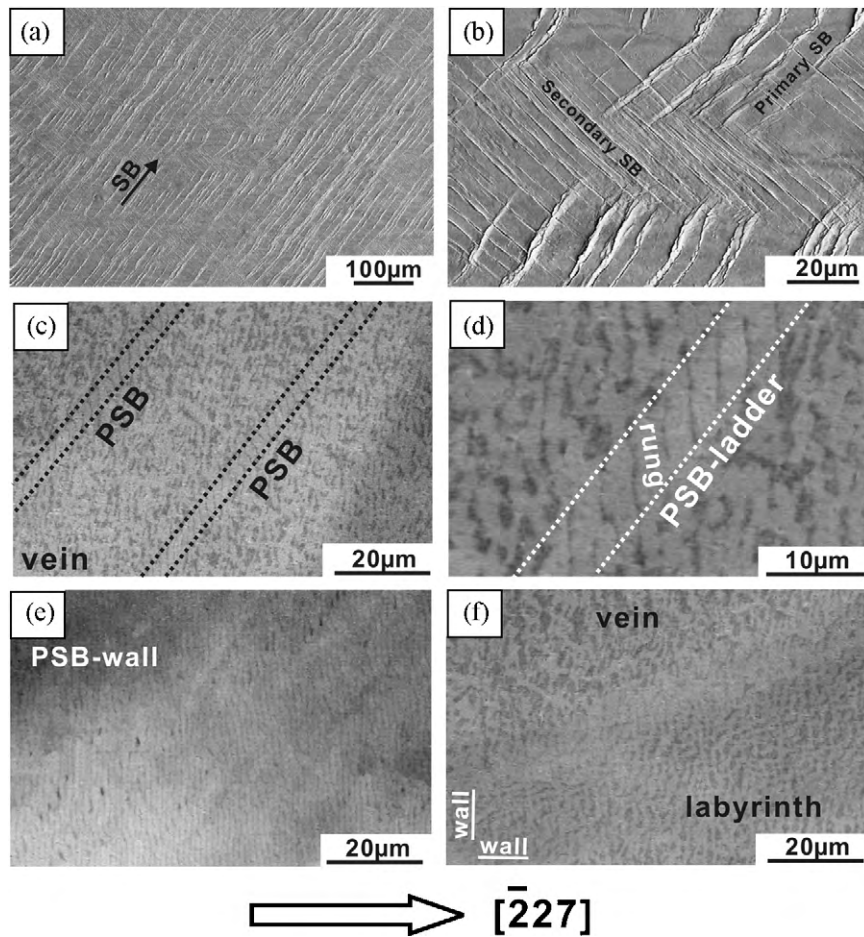


Fig. 3. Surface slip morphologies and dislocation arrangements of $[\bar{2} 27]$ Au single crystal at plastic strain amplitude of $\gamma_{pl} = 2.22 \times 10^{-3}$. (a) and (b) primary and secondary SBs; (c) and (d) two-phase structure and PSB ladder; (e) and (f) PSB-wall and labyrinth structures.

wall and labyrinth. These walls are different from the previously mentioned ladder walls. Actually, they result from the mutual locking of ladder walls. Accordingly, these new wall structures still reserve some features of the ladder wall structures, including the wall thickness and the channel width; however, the PSB height is changed. Some local regions in Au single crystal are full of the well-developed wall structures (see Fig. 3(e)). Besides the wall structure, the labyrinth structure is another complex dislocation arrangement seen in Au single crystal. Ackermann et al. [18] established a transition from dislocation ladders to labyrinth structure within the plateau. Recently, with regard to the formation of labyrinth structure, the present authors [19] gave a new interpretation based on the orientation effects. As shown in Fig. 3(f), the labyrinth structure consists of two sets of mutual perpendicular walls, whose habit planes are (001) and (100), respectively. The formation of the labyrinth structure results from the interaction between the critical secondary slip system and primary slip system. The reason can be expressed as follows [19]: single dislocations have their respective slip systems $(111)[\bar{1}01]$ and $(\bar{1}11)[101]$. However, the labyrinth walls formed by the dislocation reaction will move along the shear direction [001] and the corresponding shear systems are (100)[001] and (001)[100], respectively. It should be emphasized that the shear system only aims at the dislocation arrangements and reflects the result of the group activities, which does not change single dislocation movement along the slip system. The PSB-wall and labyrinth structure does not appear in Au single crystals cyclically deformed at $\gamma_{pl} = 1.11 \times 10^{-3}$ because the applied strain amplitude $\gamma_{pl} = 1.11 \times 10^{-3}$ is not high enough to activate the secondary slip system.

The above series of results show that the cyclic deformation behaviors of Au single crystals including the cyclic hardening curves, plateau behavior, slip morphologies and dislocation arrangements are very similar to those of Cu, Ni and Ag single crystals, which can be regarded as the most important and fundamental judgment on fcc single crystal in our series of studies [12,14]. Wang [20] summarized the cyclic deformation behaviors of various fcc metals in terms of the SFE values. The effect of the SFE on cyclic deformation behaviors of various fcc crystals is reflected by the change of slip modes. High-SFE materials demonstrate the wavy-slip behavior, in which cross-slip will easily occur and planar array of dislocations will be destroyed. On the contrary, in the fcc materials with low SFE, cross-slip is difficult and the planar array of dislocations becomes the main feature.

If taking the SFE as a criterion [20–23], the similarity in the cyclic deformation behaviors of Ni, Cu, Ag and Au single crystals can be well summarized, as shown in Table 1. Firstly, the above cyclically saturated fcc single crystals show obvious plateau behavior corresponding to the formation of PSB-ladder structure. Secondly, the plateau stresses of these fcc single crystals are different from each other, however, the ratio of the plateau stress to the shear modulus [24] is roughly equivalent. In addition to τ_s/G , the ratio G/γ_{sf} of the shear modulus to the SFE also can be regarded as a constant closely related to the formation of PSBs. The present authors [12] have found that only when G/γ_{sf} is about in the range of $(1-2) \times 10^{12} \text{ m}^{-1}$, the classical PSB-ladder structure is able to appear. In fact, G/γ_{sf} and τ_s/G characterize the width of extended dislocation and the trap distance of dipole, respectively. When the trap distance d_{trap} is less than the critical trap distance $d_{critical}$, a relatively stable dipole segment may form. Together with the width of extended dislocation, they are closely linked with the evolution of dislocation configurations.

Therefore, it is reasonable to suggest that the two parameters τ_s/G and G/γ_{sf} play important roles in the evolution and formation of dislocation patterns, which will be expected to make more

thinking and discussion around them [25]. In addition, the great advantage of Au single crystal is its excellent resistance to corrosion, therefore, Au single crystal will offer more conveniences in studying environmental effects on CSS behavior, strain localization, PSB variations during cyclic deformation [26] and fatigue fracture as compared to Cu [27] and other fcc single crystals.

4. Conclusions

- (1) The CSS curve of [227] Au single crystal shows an obvious plateau behavior at least in the strain range of 1.11×10^{-3} to 2.22×10^{-3} . The plateau stress of Au single crystals is about 23.4 MPa, which is located between those of Cu and Ag single crystals. In cyclically saturated Au single crystal, not only classical vein and PSB-ladder structures have formed, but also the wall and labyrinth structures can be found, which are likewise similar to those of Cu, Ni and Ag single crystals.
- (2) After summarizing the cyclic deformation behaviors of Cu, Ni, Au and Ag single crystals, it can be found that two basic parameters τ_s/G and G/γ_{sf} play important roles in the evolution and formation of dislocation patterns. In fact, G/γ_{sf} and τ_s/G characterize the width of extended dislocation and the trap distance of dipole, respectively. Only when the values of both parameters are within a certain range, the classical PSB-ladder structure is able to appear.

Acknowledgements

The authors are grateful to H.H. Su, W. Gao, Q.Q. Duan and H.F. Zou for their assistance in the fatigue experiments and dislocation observations. This work was financially supported by the “Hundred of Talents Project” of Chinese Academy of Sciences, the National Outstanding Young Scientist Foundation under grant no. 50625103, and the National Basic Research Program of China under grant no. 2010CB631006.

References

- [1] N. Thompson, N. Wadsworth, N. Louat, *Philos. Mag.* 1 (1956) 113.
- [2] A.T. Winter, *Philos. Mag.* 30 (1974) 719.
- [3] J.M. Finney, C. Laird, *Philos. Mag.* 31 (1975) 339.
- [4] H. Mughrabi, *Mater. Sci. Eng.* 33 (1978) 207.
- [5] H. Mughrabi, K. Herz, F. Ackermann, *Proceedings, 4th International Conference on the Strength of Metals and Alloys*, vol. 3, Nancy, 1976, p. 1244.
- [6] J.C. Grosskreutz, H. Mughrabi, in: A.S. Argon (Ed.), *Constitutive Equations in Plasticity*, MIT Press, Cambridge, MA, 1975, p. 251.
- [7] P. Neumann, *Z. Metallkd.* 59 (1968) 927.
- [8] B.D. Yan, A. Hunsche, P. Neumann, C. Laird, *Mater. Sci. Eng.* 79 (1986) 9.
- [9] H. Mughrabi, F. Ackermann, K. Herz, in: J.T. Fong (Ed.), *Fatigue Mechanisms*. ASTM STP 675, ASTM, Philadelphia, 1979, p. 69.
- [10] C. Blochwitz, U. Veit, *Cryst. Res. Technol.* 17 (1982) 529.
- [11] P. Li, Z.F. Zhang, S.X. Li, Z.G. Wang, *Acta Mater.* 56 (2008) 2212.
- [12] P. Li, Z.F. Zhang, S.X. Li, Z.G. Wang, *Scr. Mater.* 59 (2008) 730.
- [13] P. Li, Z.F. Zhang, S.X. Li, Z.G. Wang, *Philos. Mag.* 89 (2009) 2903.
- [14] P. Li, Z.F. Zhang, X.W. Li, S.X. Li, Z.G. Wang, *Acta Mater.* 57 (2009) 4845.
- [15] D. Kuhlmann-Wilsdorf, *Metall. Mater. Trans. A* 35 (2004) 5.
- [16] P. Hahner, *Appl. Phys. A* 63 (1996) 45.
- [17] O. Vorren, N. Ryum, *Acta Metall.* 36 (1988) 1443.
- [18] F. Ackermann, L.P. Kubin, J. Lepinoux, H. Mughrabi, *Acta Metall.* 32 (1984) 715.
- [19] P. Li, Z.F. Zhang, S.X. Li, Z.G. Wang, *Acta Mater.* 58 (2010) 3281.
- [20] Z.R. Wang, *Philos. Mag.* 84 (2004) 351.
- [21] D.Z. Yang, *Dislocation and Metal Strengthening Mechanism*, Harbin Institute of Technology Press, Harbin, 1991.
- [22] M. Rester, C. Motz, R. Pippin, *Scr. Mater.* 58 (2008) 187.
- [23] L.E. Murr, *Interfacial Phenomena in Metals and Alloys*, Addison-Wesley, Reading, MA, 1975.
- [24] Z.S. Hou, G.X. Lu, *Principles of Metallography*, Shanghai Scientific & Technical Publishers, Shanghai, 1990.
- [25] P. Li, Z.F. Zhang, S.X. Li, Z.G. Wang, *Prog. Mater. Sci.* Submitted.
- [26] J.M. Finney, C. Laird, *Mater. Sci. Eng.* 54 (1982) 137.
- [27] D.E. Witmer, G.C. Farrington, C. Laird, *Acta Metall.* 35 (1987) 1895.